

Large Uncertainty in Permafrost Carbon Stocks due to Hillslope Soil Deposits

Eitan Shelef¹, Joel C. Rowland², Cathy J. Wilson², G.E. Hilly³, Umakant

Mishra⁴, Garrett L. Altmann² and Chien-Lu Ping⁵

¹ Earth and Environmental Science

Division, Los Alamos National Laboratory,
NM, now at the Department of Geology and
Environmental Science, University of
Pittsburgh, PA

² Earth and Environmental Science

Division, Los Alamos National Laboratory,
NM

This article has been accepted for publication and undergone full peer review but has not been through the copyediting, typesetting, pagination and proofreading process, which may lead to differences between this version and the Version of Record. Please cite this article as doi: 10.1002/2017GL073823

Northern circumpolar permafrost soils contain more than a third of the global Soil Organic Carbon pool (SOC). The sensitivity of this carbon pool to a changing climate is a primary source of uncertainty in simulation-based climate projections. These projections, however, do not account for the accumulation of soil deposits at the base of hillslopes (hill-toes), and the influence of this accumulation on the distribution, sequestration, and decomposition of SOC in landscapes affected by permafrost. Here we combine topographic models with soil-profile data and topographic analysis to evaluate the quantity and uncertainty of SOC mass stored in perennially frozen hill-toe soil deposits. We show that in Alaska this SOC mass introduces an uncertainty that is $> 200\%$ than state-wide estimates of SOC stocks (77 PgC), and that a similarly large uncertainty may also pertain

³ Department of Geological and

Environmental sciences, Stanford
University, CA

⁴ Environmental Science Division,

Argonne National Laboratory, IL

⁵ SNRE Agriculture and Forestry

Experiment Station, University of Alaska
Fairbanks, AK.

at a circumpolar scale. Soil sampling and geophysical-imaging efforts that target hill-toe deposits can help constrain this large uncertainty.

Accepted Article

1. Introduction

The thawing of permafrost soils in the Arctic may release vast amounts of carbon (C) to the atmosphere and induce a positive feedback between increasing temperature, thawing, and further carbon release [Zimov *et al.*, 2006; Schuur *et al.*, 2015; Harden *et al.*, 2012].

Current estimates for northern circumpolar areas suggest that seasonally thawed shallow soils contain ~ 500 Pg C, and ~ 800 Pg C are stored in deeper perennially frozen soils [Hugelius *et al.*, 2014]. This deeper repository of C has accumulated over $\sim 10^3 - 10^5$ years from seasonal vegetation growth followed by die-off and burial, such that SOC is incorporated into deep and perennially frozen soil where SOC decomposition rates are extremely slow [Tarnocai *et al.*, 2009; Zimov *et al.*, 2006; Michaelson *et al.*, 1996; Schuur *et al.*, 2008; Harden *et al.*, 2012; Elberling *et al.*, 2013]. Coupled land-climate models that account for permafrost thawing predict that permafrost soils will become a major carbon source of several to hundreds Pg C over the next century [Zhuang *et al.*, 2006; Koven *et al.*, 2011; Harden *et al.*, 2012]. These models, however, are associated with a large uncertainty that is primarily an outcome of the uncertainty in permafrost SOC quantity and distribution [Burke *et al.*, 2012; Mishra *et al.*, 2013; Hugelius *et al.*, 2014].

The feedback between the thawing of permafrost SOC and Earth's climate motivated substantial efforts to evaluate the quantity and distribution of this frozen C reservoir through sampling and spatial interpolation [e.g., Michaelson *et al.*, 1996; Ping *et al.*, 2005; Zimov *et al.*, 2006; Ping *et al.*, 2008; Tarnocai *et al.*, 2009; Harden *et al.*, 2012; Jorgenson *et al.*, 2013; Mishra *et al.*, 2013; Hugelius *et al.*, 2014]. These efforts appreciably improved the quantification of permafrost SOC, but estimates remain poorly constrained in areas of

considerable topographic relief such as Arctic foothills, uplands, and mountains, as well as for SOC stocks at depth larger than 3 meters [Mishra *et al.*, 2013; Hugelius *et al.*, 2014]. This data gap, an outcome of sampling difficulties in these remote areas, may disrupt the assessment of permafrost SOC stored in hillslope-scale repositories.

Accumulation of thick soil deposits at hill-toe position in permafrost environments results from downslope soil transport through soil creep and fluvial processes, as well as accumulation of locally produced organic material [Sellmann, 1967; Hamilton *et al.*, 1988; Yoo *et al.*, 2005; Berhe *et al.*, 2007; Johnson *et al.*, 2013]. These processes affect SOC distribution and sequestration because they can deposit SOC at the base of the hill (i.e., the hill-toe, which includes the toe-slope and foot-slope of the catena pedosequence, Figure 1) where low SOC decomposition rates may prevail [e.g., Berhe *et al.*, 2012]. In temperate climates, for example, downslope soil transport likely sequesters a globally meaningful quantity of SOC [Yoo *et al.*, 2005; Berhe *et al.*, 2007]. This quantity, however, strongly depends on the rate of SOC decomposition during transport and within buried deposits as well as on the rate of soil transport down the hillslope and into the riverine system [Yoo *et al.*, 2005; Berhe *et al.*, 2007] (Figure 1a,b). In permafrost regions, large SOC quantities may be sequestered into perennially frozen soils within hill-toe deposits (Figure 1b) due to a combination of low SOC decomposition rates in the active layer (i.e., the mobile upper soil that thaws every summer) when saturated [Knoblauch *et al.*, 2013; Elberling *et al.*, 2013; Schädel *et al.*, 2014], and the extremely low decomposition rates in the perennially frozen soil that underlies it [Zimov *et al.*, 2006; Schuur *et al.*, 2008; Tarnocai *et al.*, 2009; Harden *et al.*, 2012; Knoblauch *et al.*, 2013; Elberling *et al.*, 2013].

Further, the high downslope soil-transport rates documented over high latitude hillslopes [Oehm and Hallet, 2005], and the low flux of sediments to Arctic rivers [Syvitski, 2002; Gordeev, 2006], suggest that deep SOC stocks may accumulate at hill-toe positions in high latitude areas. Such soil accumulation is evident by general thickening of soil deposits at concave-up hill-toe locations [Wu, 1984; Pewe, 1989; Ping *et al.*, 2005; Sellmann, 1967; Hamilton *et al.*, 1988]. In the Fox Permafrost Tunnel, AK, for example, > 15m of deposits accumulated at a hill-toe position [Sellmann, 1967; Hamilton *et al.*, 1988]. Even though the effects of vertical soil mixing, due to cryoturbation, on SOC burial and storage in lower active layer and upper permafrost have been well explored [Michaelson *et al.*, 1996; Bockheim, 2007; Koven *et al.*, 2011; Ping *et al.*, 2015], the accumulation and burial of SOC at hill-toe positions has gone largely unaccounted in areas affected by permafrost.

The objective of this study is to evaluate the quantity and uncertainty of SOC mass stored in perennially frozen hill-toe soil deposits. To do so, we utilized the high-quality of topographic, glacial history, and soil-profile data in Alaska, combined with modeled topography, to explore the contribution of perennially frozen hill-toe deposits to the uncertainty in SOC estimates in Alaska, and by extension, in the entire northern circumpolar area (i.e., Lat > 50° North).

2. Method

2.1. Approach

To evaluate the mass of SOC stored in perennially frozen hill-toe deposits, we combined soil-profile data with topographic modeling and landscape classification. Our estimates rely on simplified geometric representations of hillslope topography, that in part rely on

a slope dependent soil transport model [e.g., *Culling*, 1963; *Govers et al.*, 1994; *Dietrich et al.*, 1995; *Yoo et al.*, 2005; *Bogaart et al.*, 2003; *Oehm and Hallet*, 2005]. Such a model predicts topographic convexity at hill-tops and concavity at hill-bottoms, where soil erosion and deposition take place, respectively. To evaluate the validity of modeled topography we explored whether this topographic pattern is indeed common in Alaska, and also measured soil depth in hill-top and hill-toe locations (Section 2.2) to corroborate published data [i.e., *Sellmann*, 1967; *Wu*, 1984; *Pewe*, 1989; *Ping et al.*, 2005]. We then evaluated the aerial extent (A [m^2]) of hilly soil-mantled terrain affected by permafrost (hereafter HSP terrain) by combining a topographic classification [*Meybeck et al.*, 2001] with permafrost and Normalized Difference Vegetation Index (NDVI) datasets (Section 2.3). We explored the thickness and SOC density (C_r [kg/m^3]) of hill-toe deposits by querying soil-profile datasets in HSP terrain in Alaska (Section 2.4, SI). The soil depth (H [m]) and hillslope relief (R [m]) associated with these soil-profiles were then used to constrain the aforementioned topographic models that were used to calculate the mean thickness (\bar{H}_p [m]) of perennially frozen hill-toe deposits (Sections 2.5, 2.6, SI). We combined this thickness, SOC density, and area of HSP terrain to approximate the volume (V [m^3]) of perennially frozen hill-toe deposits in Alaska and the mass of SOC (C_t [g]) stored in these deposits. To put our findings in a circumpolar context, we apply a similar analysis over the northern circumpolar area.

2.2. Topographic and soil depth analysis in Alaska

We used landscape curvature to explore whether the lower portion of hillslopes in Alaska is associated with a concave-up topography characteristic of depositional hillslope settings

[e.g., *Culling*, 1963; *Andrews and Hanks*, 1985; *Rosenbloom et al.*, 2001; *Yoo et al.*, 2005; *Berhe et al.*, 2007]. To do so, we mapped the topographic curvature over a smoothed digital elevation model (DEM) of Alaska (~ 50 m lateral resolution, SI) and explored the location and fraction of DEM pixels with positive curvature (Figure 1d, SI). To evaluate the heterogeneity in topographic curvature we also computed the fraction of concave-up DEM pixels across HSP areas of different permafrost categories. Whereas published data suggests that soil thickness increases in hill-toe positions at temperate and permafrost setting [e.g., *Sellmann*, 1967; *Wu*, 1984; *Pewe*, 1989; *Yoo et al.*, 2005; *Ping et al.*, 2005; *Berhe et al.*, 2007], we further explored this by sampling soil depths along a hill-top to hill-toe transect in the Seward Peninsula (Figure 1e, SI). In a location at the central Seward Peninsula (Lat, Lon: [65.43064256, -164.6769601], SI) we also dug into a gully bank at a hill-toe location to record the depth of hill-toe deposits.

2.3. Evaluating the extent of hilly soil-mantled terrain affected by permafrost (HSP terrain)

To approximate the area of HSP terrain we jointly analyzed topographic (GTOPO30 DEM [USGS, 1996]), NDVI [CAVM Team, 2003; *Walker et al.*, 2002], soil profile [*Mishra et al.*, 2017a], and permafrost zonation [*Brown et al.*, 2014] maps (Figure 2). We defined hilly terrain following the DEM (GTOPO30) based classification of *Meybeck et al.* [2001] that is used by the Circumpolar Arctic Vegetation Map team [CAVM Team, 2003]. We assumed that the joined classes of hills and low mountains [*Meybeck et al.*, 2001] appropriately represent hilly terrain. Of the selected DEM pixels, we identified those that likely represent soil-mantled terrain by querying pixels whose NDVI value exceeds a threshold

of 0.39 (computed by joined analysis of NDVI and soil-profile dataset, SI). This relies on the assumption that high NDVI corresponds with high vegetation coverage and associated soil [e.g., *Walker et al.*, 1995; *Hodkinson et al.*, 2003, SI]. From these pixels we then identified those that are mapped within permafrost areas [*Brown et al.*, 2014], and computed the HSP area by weighting the cumulative area of pixels in each permafrost category by the associated percentage of permafrost cover ($95 \pm 5\%$, $70 \pm 20\%$, $30 \pm 20\%$ and $5 \pm 5\%$ for continuous, discontinuous, sporadic, and isolated permafrost cover, respectively [after *Brown et al.*, 2014]). We computed the uncertainty in HSP area from the uncertainty in elevation and permafrost cover (SI).

2.4. Quarrying soil profiles

To extract information on the depth and SOC density of perennially frozen hill-toe deposits, we combined topographic analysis with the location and depth of soil profiles in Alaska. Our analysis relies on the Alaska soil survey dataset because it captures various landscape positions compared to other permafrost regions [*Ping et al.*, 2008; *Mishra and Riley*, 2012; *Michaelson et al.*, 2013] and facilitates a synthesis with high resolution topographic [e.g., *Mishra and Riley*, 2014] and past glaciation datasets [i.e., *Bundtzen et al.*, 2011]. The soil-profile dataset compiled by *Mishra et al.* [2017b], contains 584 georeferenced soil profiles which includes data from *Michaelson et al.* [2013]. To explore whether past glaciation is associated with soil heterogeneity we used a Kolmogorov-Smirnov test to compare the permafrost SOC density between soil profiles in and out of areas glaciated in the Pleistocene [*Bundtzen et al.*, 2011]. To identify soil profiles that likely sample perennially frozen hill-toe deposits in HSP terrain we screened the soil-profile dataset for profiles

in HSP areas (Section 2.3) that include a permafrost layer (i.e., below the active layer) over a sloping topography (to avoid valleys and planes) of positive curvature (indicative of concave up topography characteristic of hill-toes; Figure 1, SI). We computed slope and curvature from a smoothed ~ 50 m DEM of Alaska and used conservative slope and curvature thresholds (1.66° , -0.0019 m $^{-1}$, respectively, SI) that account for propagation of uncertainty in elevation. For each of the selected profiles, we manually measured the relief between the profile location and the hill-top, and used it to calculate the ratio (H/R) between the thickness of hill-toe deposits (H) and hillslope relief (R , Figure 1b). We used these ratios to constrain the depth of hill-toe deposits with a topographic model (Section 2.5, SI), and the SOC density in the permafrost portion of the profiles to evaluate the quantity of permafrost SOC in these deposits.

2.5. Evaluating SOC quantities through modeled hill-slope topography

To compute SOC quantities in HSP terrain over Alaskan and circumpolar scales we evaluated the thickness of perennially frozen hill-toe deposits averaged over the entire hillslope area. This mean thickness (\bar{H}_p [m]) is computed from the elevation difference between the recent topography (i.e., final profile), and the paleo-topography prior to initiation of soil transport and accumulation (i.e., initial profile, Figures 1c, 3f-g). For generality, these profiles are represented by two idealized non-dimensional geometries (Figure 3f-g): (a) linear, due to its simplicity, and (b) sigmoidal (based on a periodic function), which closely resembles the current topography (Figure 1). The non-dimensional profile elevation and distance (z^* , x^* , respectively) are scaled by the profile's length and final relief (R). The dimensionless elevation of the initial profile is computed such that at the hill-toe, the non-

dimensional elevation difference between the initial and final profiles (z_i^* , z_f^* , respectively) equals a prescribed non-dimensional soil depth ($H^* = H/R$, Figure 1b). The geometry of the sigmoidal profile is also consistent with the geometry produced by a diffusive soil-creep model with no flux boundary conditions [e.g., *Culling*, 1963; *Andrews and Hanks*, 1985; *Yoo et al.*, 2005] (Figures 1c, 3g). The non-dimensional mean thickness of perennially frozen hill-toe deposits (\bar{H}_p^*) is computed from the difference between $z_f^*(x^*)$ and $z_i^*(x^*)$, and accounts for the non dimensional thickness of the active layer ($a^* = a/R$):

$$\bar{H}_p^* = \int_0^1 z_f^*(x^*) - z_i^*(x^*) - a^* dx^*. \quad (1)$$

The integrand is set to zero at locations where the thickness of deposits is smaller than that of the active layer (i.e, $a^*(x^*) > z_f^*(x^*) - z_i^*(x^*)$). The dimensional mean thickness of perennially frozen deposits (\bar{H}_p [m]), for a given relief value is thus $\bar{H}_p = R\bar{H}_p^*$. The volume (V [m^3]) and SOC mass (C_t [kg]) stored in perennially frozen hill-toe deposits over a terrain of relief R [m] and area A [m^2] are approximated as

$$\begin{aligned} V &= AR\bar{H}_p^* = A\bar{H}_p, \\ C_t &= C_r V. \end{aligned} \quad (2)$$

Where C_r [kg/m^3] is the SOC density of perennially frozen hill-toe deposits (extracted from the aforementioned soil-profiles).

2.6. Constraining hill-toe soil thickness with soil-profile data

Estimates of SOC mass (C_t) in Equation 2 can rely on the mean thickness (\bar{H}_p [m]) and SOC density (C_r [kg/m^3]) of perennially frozen hill-toe deposits. To evaluate C_t

directly from the soil-profile dataset, we used the H/R value (Figure 1b) of each hill-toe soil profile to model the initial and final topography of the hillslope upslope of this profile for each one of the idealize profile geometries. We calculated \bar{H}_p (Equation 1) using the measured a and R values (Figure 1b) associated with this soil profile. Assuming that the measured soil profiles are representative of HSP terrain, C_t over this terrain can be approximated via Equation 2, where A is the area of HSP terrain (Section 2.3), and C_r and \bar{H}_p are representative values based on the soil profiles data. To account for the empirical distributions of C_r , \bar{H}_p and A , we computed V , C_t and their uncertainty with Equation 2 through a Monte-Carlo simulation (10^4 iterations) where the values of C_r , \bar{H}_p , and A are randomly sampled from these distributions.

An alternate approach that accounts for spatial changes in R and H assumes that the ratio between deposit thickness and hillslope relief (H/R) remains the same such that the thickness of deposits covaries with relief. This assumption relies on the coarse scaling of H and R in the analyzed soil profiles (SI), and on the constant H/R produced when diffusive soil transport processes [i.e., *Culling*, 1960, 1963] operate over the same time scale and with no soil flux out of the hill-toe. To evaluate SOC quantities based on this assumption we computed the distribution of local relief across HSP terrain over a circular area of 3 km radius that encompasses > 1 hillslope lengths [e.g., *McNamara et al.*, 1999; *Crawford and Stanley*, 2014] (Figure 1, SI). We then used these relief values (Figure 3e) to approximate the volume of perennially frozen hill-toe deposits:

$$V = \sum_{j=1}^{j=n} \bar{H}_{pj} A_j. \quad (3)$$

Where n is the number of unique local relief values within the area of HSP terrain ($n > 790$ where the relief is rounded to 1 m intervals), j is the index associated with a given relief value (R_j), \bar{H}_{pj} is the \bar{H}_p value computed for this R_j (i.e., Equation 2), and A_j is the cumulative area of HSP pixels with such local relief. This estimate is conservative in that it relies on relief values measured from a $\sim 1\text{km}$ GTOPO30 DEM that generally underestimates relief [Zhang *et al.*, 1999]. Here, the Monte-Carlo simulation used to compute the value and uncertainty of V and C_t also accounts for the area (A_j) associated with different relief values (SI).

Whereas our analysis is primarily focused on Alaska, where the density and quality of data is generally high compared to most high latitude areas, we also attempted to estimate the potential contribution of perennially frozen hill-toe deposits to the uncertainty in circumpolar SOC mass. To do so, we used circumpolar permafrost distribution, topographic and NDVI data to constrain the extent and relief of circumpolar HSP terrain. We estimated the deposits depth and SOC density by making the assumption that the soil profiles measured in Alaska are representative over a circumpolar scale. Whereas this assumption is essential to put our findings in a circumpolar context, it adds an unquantified component of uncertainty to this circumpolar permafrost distribution due to the potential variability in soil formation and accumulation factors between Alaska and other circumpolar terrains.

3. Results

3.1. Topographic and soil depth analysis in Alaska

Topographic analysis (over a ~ 50 m DEM, Section 2.2) suggests that concave up topography, where soil deposition and accumulation is expected, is common at the base of hillslopes (Figure 1d) and covers $\sim 54\%$ of the HSP area in Alaska. This fraction is similar for HSP areas in different permafrost categories (55, 53, 57, and 56% for continuous, discontinuous, sporadic, and isolated, respectively). The accumulation of soil at concave hill-toe locations is supported by measurements of soil thickness along a hill-top to hill-toe transect in the Seward Peninsula (Figure 1e, Lat, Lon: 65.026660,-166.16686, SI). The sampling and drilling depth in the upper three locations was hampered by rock fragments (4-7 cm diameter) that are likely associated with proximity to bedrock. However, at the lowermost location the drill-bit freeze-stuck at a depth of 177 cm (53 cm in thawed soil and 124 cm in frozen soil) without encountering rock clasts. Hence, the depth to bedrock is likely > 177 cm. Deep frozen hill-toe deposits (> 229 cm) were also measured at a different location in the Seward Peninsula (Lat, Lon: [65.43064256,-164.6769601], SI).

3.2. Extent and relief of HSP terrain in Alaska

The estimated area (A) of HSP terrain in Alaska is $4.1_{-1.17}^{+1.33} \times 10^5$ km 2 ; this area is approximately 45% of the permafrost-covered area in Alaska. The local relief of HSP terrain over a 3 km radius is 291_{-220}^{+319} m (uncertainties are reported based on the mean, 5, and 95 percentiles unless stated otherwise; Figure 3e). HSP terrain generally does not overlap with the extent of Late Wisconsinan glaciation, and partly overlaps with that of maximal Pleistocene glaciation (SI).

3.3. Analysis of soil profiles and their location

Topographic analysis of soil-profile locations in Alaska shows that out of 584 soil profiles, only 16 profiles (~3%) sampled permafrost deposits in hill-toe locations over HSP terrain (Figure 2a, Table S1). The SOC density (Figure 3d) in the permafrost portion of these 16 profiles is $45.8^{+76.2}_{-38.9}$ [kg/m³]. The ratio between the thickness of hill-toe deposits to hillslope relief (H/R) for these 16 soil sampling sites as well as the two hill-toe deposits we sampled in the Seward Peninsula is $0.037^{+0.048}_{-0.018}$ (Figure 3c). The thickness of the active layer in these 18 samples is $0.43^{+0.54}_{-0.35}$ m, and the hillslope relief is 37^{+29}_{-23} m (SI). A Kolmogorov-Smirnov test for comparison of permafrost SOC density between soil profiles in and out of areas glaciated in the Pleistocene failed to reject the null hypotheses that the samples come from the same distribution (for a significance level of $\alpha = 0.05$).

3.4. The mass of permafrost SOC at hill-toe locations in Alaska

Estimates that rely on the assumption that the H and R values of soil sampling sites are representative of HSP terrain in Alaska (Figure 3a) result in mean C_t values of ~ 2 - 3 Pg C for the two idealized profile geometries with a maximal uncertainty of ~ 12 Pg C (current SOC estimate for Alaska is 77 Pg C, [Mishra and Riley, 2012]). Estimates that rely on the assumption that the thickness of hill-toe deposits scales with hillslope relief (i.e., Equation 3, Figure 3b) results in mean C_t values of $\sim 65 - 85$ Pg C, with a maximal uncertainty of > 200 Pg C.

3.5. Circumpolar estimates

The estimated area (A) and local relief of circumpolar HSP terrain is $3.968^{+1.571}_{-1.353} \times 10^6$ km² (Figure 2), and 243^{+261}_{-181} m, respectively (Section 2.3). C_t estimates that rely on the assumption that the H and R values measured for soil sampling sites in Alaska are

representative of circumpolar HSP terrain result in mean C_t values of ~ 25 to ~ 35 Pg C for the linear and sigmoidal profile geometries, respectively, with a maximal uncertainty of > 100 Pg C (SI). The mean volume of hill-toe deposits is ~ 530 and ~ 790 km³ for the linear and sigmoidal profile geometries, respectively. For comparison, the volume of delta deposits of major circumpolar rivers is 3514 km³ over an area of 75800 km² [Hugelius *et al.*, 2014]. C_t estimates that rely on the assumption that the thickness of hill-toe deposits scales with the hillslope relief (i.e., Equation 3) result in mean C_t values of ~ 550 and ~ 720 Pg C for the linear and sigmoidal profile geometries, respectively, with a maximal uncertainty of > 2000 Pg C (SI). In that case, the mean overall volume of hill-toe deposits ranges from $\sim 12,000$ to $\sim 16,000$ km³, which is up to several times more than the aforementioned volume of delta deposits. The maximal uncertainty of > 2000 Pg C is similar to estimates of global SOC mass in depths of zero to three meters (2000-3000 Pg C, [Schuur *et al.*, 2008; Tarnocai *et al.*, 2009]).

3.6. Uncertainty contribution

Our results point at a large uncertainty in hillslope scale SOC stocks. This uncertainty is primarily influenced by the assumptions we make; the assumption that the depth of hill-toe soil profiles does or does-not scale with hillslope relief causes a factor of > 20 difference in mean C_t estimates (Figure 3a-b). The variance in soil profile data also contributes to the reported uncertainty. For example, setting both the SOC density (C_r) and the dimensionless deposits depth (H/R) at their mean value in the Monte-carlo procedure reduces the uncertainty in C_t estimates by a factor of ~ 6 for the two profile geometries.

Differences between the assumed hillslope geometry cause a factor of \sim 1-2 difference in mean C_t estimates (Figures 3a-b, 3f-g).

4. Discussion

4.1. SOC storage in perennially frozen hill-toe deposits

Our results suggest that perennially frozen hill-toe deposits can store considerable SOC stocks due to their extent, thickness, and SOC density. The concave up topography at the lower portion of hillslopes (Figure 1d, 1e) is consistent with deposition and soil accumulation at hill-toes (Figures 1a, 1b) [e.g., *Andrews and Hanks*, 1985; *Rosenbloom et al.*, 2001; *Berhe et al.*, 2007] and contrasts with the convex shape typical of steady state hillslopes where sediments do not accumulate at the hill-toe [*Culling*, 1960, 1963].

The accumulation of soil deposits at hill-toe positions is supported by our measurements (Figures 1e, Section 3.1, SI), as well as by published measures of soil depths in different slope locations across Alaska [e.g., *Sellmann*, 1967; *Hamilton et al.*, 1988; *Pewe*, 1989; *Wu*, 1984; *Ping et al.*, 2005]). The SOC density measured in the 16 soil profiles at hill-toe locations ($45.8^{+76.2}_{-38.9}$ [kg/m³]; Figure 3d, Table S1) is higher than that measured in temperate climates (typically < 10 [kg/m³] for deposits deeper than 60 cm [*Yoo et al.*, 2005]), and likely reflects low SOC decomposition rate in permafrost conditions (Figure 1) [e.g., *Tarnocai et al.*, 2009; *Zimov et al.*, 2006; *Michaelson et al.*, 1996; *Schuur et al.*, 2008; *Harden et al.*, 2012; *Elberling et al.*, 2013].

4.2. Uncertainty in SOC quantities stored in perennially frozen hill-toe deposits

Estimates of SOC mass stored in perennially frozen hill-toe deposits alone vary from few percents to more than double of current SOC estimates (Figure 3a-b). This uncertainty deviates from that reported by *Hugelius et al.* [2014] for perennially frozen soil within the upper 3 meters in circumpolar permafrost terrain (13% uncertainty for an overall estimate of 822 Pg C overall [computed from *Hugelius et al.*, 2014]). The deviation in uncertainty estimates primarily occurs because our estimate accounts for hill-toe deposits that may exceed 3 m depth, where the high uncertainty we report primarily stems from: (a) lack of sufficient field measures of hill-toe deposits depth; and (b) the small number of hill-toe soil profiles ($N = 18$; 16 from the soil dataset and 2 from this study) and the skewness of soil properties within this small dataset (i.e., Figures 3c-d, SI). The conservative SOC estimate (mean values of $\sim 2 - 3$ and $\sim 26 - 36$ Pg C in perennially frozen hill-toe deposits in Alaska and Circumpolar areas, respectively) is likely overly-conservative because: (a) the volume (V) of hill-toe deposits is probably underestimated because it is unlikely that the 18 hill-toe soil profiles sample the depth of hill-toe deposits deep enough (usually less than 1.6 m); (b) this estimate relies on the assumption that the 18 hill-toe soil-profiles properly represent the thickness of hill-toe deposits elsewhere, even though the mean relief (37 m) associated with these profiles is $<16\%$ of the mean relief measured over Alaskan (291 m) and Circumpolar (243 m) HSP terrain. The alternate SOC estimate (mean values of $\sim 65 - 85$ and $\sim 550 - 720$ Pg C in perennially frozen hill-toe deposits in Alaska and Circumpolar areas, respectively) may be non-conservative in that it assumes that the thickness of hill-toe deposits (H) scales with hillslope relief (R). Whereas these

end-member estimates likely under- and over- estimate SOC mass at hill-toe deposits, they bracket potential estimates and bring forth the large uncertainty associated with hillslope-scale controls on SOC stocks. The primary components of this uncertainty (i.e., the depth, SOC density, and geometry of hill-toe deposits) can likely be reduced by soil sampling, drilling, and geophysical imaging [e.g., *Leopold et al.*, 2008; *Schrott and Sass*, 2008; *Scapozza et al.*, 2015] of the extent of hill-toe deposits along the profile of hillslopes of different relief.

Uncertainty in hill-toe SOC estimates may also arise from spatio-temporal heterogeneity in factors such as topography, hydrology, permafrost condition, and glacial history.

Whereas Late Wisconsinan Glaciation hardly overlaps with HSP terrain in Alaska (Section 3.2), and Pleistocene Glaciation do not significantly influence permafrost SOC density in soil profiles (Section 3.3), the timing of deglaciation likely influences the duration of soil accumulation and hence the thickness of hill-toe deposits. Thus, areas that were not subject to recent glaciation such as Siberia or north-west and interior Alaska will likely have thicker hill-toe deposits compared to recently deglaciated areas in Canada and north-west Eurasia [*Tarasov and Peltier*, 1997; *Svendsen et al.*, 2004; *Duk-Rodkin et al.*, 2004].

Thick hill-toe deposits are indeed reported in Boreal zones in central Alaska that were not recently glaciated [*Michaelson et al.*, 2013]. The similar fraction of concave-up HSP topography between areas of different permafrost categories (Section 3.1) hints that in Alaska, different permafrost conditions do not have a major influence on topographically induced accumulation of hill-toe deposits. However, a more detailed topographic investi-

gation is required to explore the influence of permafrost regimes on HSP topography at different scales.

Hill-toe SOC stocks can also be influenced by spatially varying factors such as cryoturbation, permafrost conditions, soil saturation, bedrock type, mineral weathering, vegetation, wild-fires, and microclimate caused by slope and aspect [Ping *et al.*, 2005; Jorgenson *et al.*, 2013]. An additional uncertainty component stems from topographic variations that differ from the assumed 2D profiles. The reported circumpolar estimates should be approached with caution because they rely on soil profiles from Alaska that may not be characteristic of the entire circumpolar. Given these multiple sources of uncertainty, the SOC quantities we computed highlight the potential SOC mass stored in perennially frozen hill-toe deposits, and point at the importance of better constraining different uncertainty sources. This can be attained through further exploration of hillslope-scale processes and SOC stocks across different environmental conditions in the context of the hillslope profile and the catena pedosequence [e.g., Ping *et al.*, 2005].

4.3. The fate of hill-toe SOC and future climate predictions

Hillslope-scale processes and SOC stocks can not only influence the uncertainty of coupled land climate models through the quantity and spatial distribution of SOC stocks [i.e., Burke *et al.*, 2012; Mishra *et al.*, 2013; Hugelius *et al.*, 2014], but also the fate of SOC in a warming climate. For example, the predicted decrease in permafrost extent over the next century [Koven, 2012] together with the high erodibility of thawed soils compared to permafrost ones [Mann *et al.*, 2010], the expected shift from snow- to rain-dominated precipitation patterns [McAfee *et al.*, 2013], and the discharge that can be generated over

the large upslope areas that drain into arctic hill-toes [McNamara *et al.*, 1999; *Crawford and Stanley*, 2014], suggest that enhanced fluvial erosion of hill-toe deposits may occur in response to a warming climate. Such erosion may increase SOC flux into rivers and oceans [e.g., *Hilton et al.*, 2015; *Tesi et al.*, 2016], where its decomposition rate may change and thus influence the global C balance. Incision by fluvial erosion may also expedite thaw rates by exposing currently buried perennially frozen hill-toe deposits to a warming atmosphere. On the other hand, climate change may also increase the accumulation rate of hill-toe deposits by increasing the length of the thaw period when the active soil layer is mobile [*Hinzman et al.*, 2005; *Oehm and Hallet*, 2005; *Schuur et al.*, 2008] and also increase its thickness [*Akerman*, 2005]. If soil deposition rates at hill-toe locations exceed those of thaw-depth increase, downslope soil-transport can continue to sequester SOC into permafrost despite the projected thaw-depth increase.

5. Summary

Synthesis of a geomorphologic model, soil-profile data, and topographic analysis suggests that the uncertainty in SOC mass stored in perennially frozen hill-toe deposits in Alaska is $> 200\%$ than current estimates of state-wide SOC mass. A similarly large uncertainty may also pertain at a circumpolar scale. This uncertainty can considerably influence recent evaluations of permafrost SOC stocks, and points at a potential underestimation in current approximations of SOC stocks. The potential influence of these SOC stocks on projections of SOC fate and land-climate interactions bring forth the importance of sampling, imaging, and modeling efforts that target hill-toe deposits, especially those aimed to constrain the thickness of these deposits.

Acknowledgments.

Data supporting our analysis is contained as tables and figures within the manuscript and supplements. The maps and soil profile data we used are publicly available through the cited map sources and publications. For specific code requests please contact Eitan Shelef (shelef@pitt.edu).

This study is part of the Next Generation Ecosystem Experiment (NGEE), which is supported by the office of Biological Research in the DOE Office of Science. Contributions of U. Mishra were supported under Argonne National Laboratory Contract No. DE-AC02-06CH11357. The authors thank Dr. Brad Goodfellow for insightful comments on an early version of this manuscript, as well as Dr. Cardenas and three anonymous reviewers for their insightful and constructive comments.

References

Akerman, H. J., Relations between slow slope processes and active-layer thickness 1972–2002, Kapp Linné, Svalbard, *Norsk Geografisk Tidsskrift*, 59(2), 116–128, 2005.

Andrews, D., and T. Hanks, Scarp degraded by linear diffusion: inverse solution for age, *Journal of Geophysical Research: Solid Earth (1978–2012)*, 90(B12), 10,193–10,208, 1985.

Berhe, A. A., J. Harte, J. W. Harden, and M. S. Torn, The significance of the erosion-induced terrestrial carbon sink, *BioScience*, 57(4), 337–346, 2007.

Berhe, A. A., J. W. Harden, M. S. Torn, M. Kleber, S. D. Burton, and J. Harte, Persistence of soil organic matter in eroding versus depositional landform positions, *Journal of Geophysical Research: Biogeosciences*, 117(G2), 2012.

Bockheim, J., Importance of cryoturbation in redistributing organic carbon in permafrost-affected soils, *Soil Science Society of America Journal*, 71(4), 1335–1342, 2007.

Bogaart, P. W., G. E. Tucker, and J. De Vries, Channel network morphology and sediment dynamics under alternating periglacial and temperate regimes: a numerical simulation study, *Geomorphology*, 54(3), 257–277, 2003.

Brown, J., O. J. Ferrians, J. Heginbottom, and E. Melnikov, Circum-arctic map of permafrost and ground-ice conditions, 2014.

Bundtzen, T., J. Harvey, R. Reger, and A. Werner, Alaska palaeo-glacier atlas (version 2), *Quaternary Glaciations-Extent and Chronology: A Closer Look*, p. 427, 2011.

Burke, E. J., I. P. Hartley, and C. D. Jones, Uncertainties in the global temperature change caused by carbon release from permafrost thawing, *The Cryosphere Discussions*, 6(2), 1367–1404, 2012.

CAVM Team, Circumpolar Arctic Vegetation Map.(1: 7,500,000 scale), Conservation of Arctic Flora and Fauna (CAFF) Map No. 1, *US Fish and Wildlife Service, Anchorage, Alaska*, 2003.

Craun, K. J., Mapping benefits from updated IfSAR data in Alaska: improved source data enables better maps, *Tech. rep.*, US Geological Survey, 2015.

Crawford, J. T., and E. H. Stanley, Distinct fluvial patterns of a headwater stream network underlain by discontinuous permafrost, *Arctic, AntArctic, and Alpine Research*, 46(2), 344–354, 2014.

Culling, W., Analytical theory of erosion, *The Journal of Geology*, 68(3), 336–344, 1960.

Culling, W., Soil creep and the development of hillside slopes, *The Journal of Geology*, 71(2), 127–161, 1963.

Dietrich, W. E., R. Reiss, M.-L. Hsu, and D. R. Montgomery, A process-based model for colluvial soil depth and shallow landsliding using digital elevation data, *Hydrological Processes*, 9(3-4), 383–400, 1995.

Duk-Rodkin, A., R. W. Barendregt, D. G. Froese, F. Weber, R. Enkin, I. R. Smith, G. D. Zazula, P. Waters, and R. Klassen, Timing and extent of Plio-Pleistocene glaciations in north-western Canada and east-central Alaska, *Developments in Quaternary Sciences*, 2, 313–345, 2004.

Elberling, B., A. Michelsen, C. Schädel, E. A. Schuur, H. H. Christiansen, L. Berg, M. P. Tamstorf, and C. Sigsgaard, Long-term CO₂ production following permafrost thaw, *Nature Climate Change*, 3(10), 890–894, 2013.

Gordeev, V. V., Fluvial sediment flux to the Arctic Ocean, *Geomorphology*, 80(1), 94–104, 2006.

Govers, G., K. Vandaele, P. Desmet, J. Poesen, and K. Bunte, The role of tillage in soil redistribution on hillslopes, *European Journal of Soil Science*, 45(4), 469–478, 1994.

Hamilton, T. D., J. L. Craig, and P. V. Sellmann, The Fox permafrost tunnel: A late Quaternary geologic record in central Alaska, *Geological Society of America Bulletin*, 100, 948–969, 1988.

Harden, J. W., et al., Field information links permafrost carbon to physical vulnerabilities of thawing, *Geophysical Research Letters*, 39(15), 2012.

Hilton, R. G., et al., Erosion of organic carbon in the Arctic as a geological carbon dioxide sink, *Nature*, 524(7563), 84–87, 2015.

Hinzman, L. D., et al., Evidence and implications of recent climate change in northern Alaska and other Arctic regions, *Climatic Change*, 72(3), 251–298, 2005.

Hodkinson, I. D., S. J. Coulson, and N. R. Webb, Community assembly along proglacial chronosequences in the high arctic: vegetation and soil development in north-west Svalbard, *Journal of Ecology*, 91(4), 651–663, 2003.

Hugelius, G., et al., Estimated stocks of circumpolar permafrost carbon with quantified uncertainty ranges and identified data gaps, *Biogeosciences*, 11(23), 6573–6593, 2014.

Johnson, K. D., J. W. Harden, A. D. McGuire, M. Clark, F. Yuan, and A. O. Finley, Permafrost and organic layer interactions over a climate gradient in a discontinuous permafrost zone, *Environmental Research Letters*, 8(3), 035,028, 2013.

Jorgenson, M. T., et al., Reorganization of vegetation, hydrology and soil carbon after permafrost degradation across heterogeneous boreal landscapes, *Environmental Research Letters*, 8(3), 035,017, 2013.

Knoblauch, C., C. Beer, A. Sosnin, D. Wagner, and E.-M. Pfeiffer, Predicting long-term carbon mineralization and trace gas production from thawing permafrost of northeast Siberia, *Global Change Biology*, 19(4), 1160–1172, 2013.

Koven, C. D., Analysis of permafrost thermal dynamics and response to climate change in the CMIP5 Earth System Models, *Journal of Climate*, 2012, 2012.

Koven, C. D., B. Ringeval, P. Friedlingstein, P. Ciais, P. Cadule, D. Khvorostyanov, G. Krinner, and C. Tarnocai, Permafrost carbon-climate feedbacks accelerate global

warming, *Proceedings of the National Academy of Sciences*, 108(36), 14,769–14,774, 2011.

Leopold, M., D. Dethier, J. Völkel, and T. Raab, Combining sediment analysis and seismic refraction to describe the structure, thickness and distribution of periglacial slope deposits at Niwot Ridge, Rocky Mountains Front Range, Colorado, USA, *Zeitschrift für Geomorphologie, Supplementary Issues*, 52(2), 77–94, 2008.

Mann, D. H., P. Groves, R. E. Reanier, and M. L. Kunz, Floodplains, permafrost, cottonwood trees, and peat: What happened the last time climate warmed suddenly in Arctic Alaska ?, *Quaternary Science Reviews*, 29(27), 3812–3830, 2010.

McAfee, S. A., J. Walsh, and T. S. Rupp, Statistically downscaled projections of snow/rain partitioning for Alaska, *Hydrological Processes*, 2013.

McNamara, J. P., D. L. Kane, and L. D. Hinzman, An analysis of an Arctic channel network using a digital elevation model, *Geomorphology*, 29(3), 339–353, 1999.

Meybeck, M., P. Green, and C. Vörösmarty, A new typology for mountains and other relief classes: an application to global continental water resources and population distribution, *Mountain Research and Development*, 21(1), 34–45, 2001.

Michaelson, G. J., C. Ping, and J. Kimble, Carbon storage and distribution in tundra soils of Arctic Alaska , USA, *Arctic and Alpine Research*, pp. 414–424, 1996.

Michaelson, G. J., C.-L. Ping, and M. Clark, Soil pedon carbon and nitrogen data for Alaska : An analysis and update., *Open Journal of Soil Science*, 3(2), 2013.

Mishra, U., and W. J. Riley, Alaska n soil carbon stocks: spatial variability and dependence on environmental factors, *Biogeosciences*, 9(9), 3637–3645, 2012.

Mishra, U., and W. J. Riley, Active-layer thickness across alaska: Comparing observation-based estimates with CMIP5 earth system model predictions, *Soil Science Society of America Journal*, 78(3), 894–902, 2014.

Mishra, U., B. Drewniak, J. Jastrow, and R. Matamala, Spatial representation of high latitude organic carbon and active-layer thickness in CMIP5 earth system models, *Geoderma*, 300, 55–63, doi:10.1016/j.geoderma.2016.04.017, 2017a.

Mishra, U., J. Jastrow, R. Matamala, and Z. Fan, Observational needs for estimating alaskan soil carbon stocks under current and future climate, *Journal of Geophysical Research: Biogeosciences*, 122(2), 415–429, 2017b.

Mishra, U., et al., Empirical estimates to reduce modeling uncertainties of soil organic carbon in permafrost regions: a review of recent progress and remaining challenges, *Environmental Research Letters*, 8(3), 035,020, 2013.

Oehm, B., and B. Hallet, Rates of soil creep, worldwide: weak climatic controls and potential feedback, *Zeitschrift für Geomorphologie, NF*, 49(3), 353–372, 2005.

Pewe, T. L., Quaternary stratigraphy of the Fairbanks area, Alaska, *US Geological Survey Circular*, 1026, 72–77, 1989.

Ping, C., G. Michaelson, E. Packee, C. Stiles, D. Swanson, and K. Yoshikawa, Soil catena sequences and fire ecology in the boreal forest of alaska, *Soil Science Society of America Journal*, 69(6), 1761–1772, 2005.

Ping, C., J. Jastrow, M. Jorgenson, G. Michaelson, and Y. Shur, Permafrost soils and carbon cycling, *Soil*, 1(1), 147, 2015.

Ping, C.-L., G. J. Michaelson, M. T. Jorgenson, J. M. Kimble, H. Epstein, V. E. Romanovsky, and D. A. Walker, High stocks of soil organic carbon in the north american arctic region, *Nature Geoscience*, 1(9), 615–619, 2008.

Rosenbloom, N. A., S. C. Doney, and D. S. Schimel, Geomorphic evolution of soil texture and organic matter in eroding landscapes, *Global Biogeochemical Cycles*, 15(2), 365–381, 2001.

Scapozza, C., L. Baron, and C. Lambiel, Borehole logging in alpine periglacial talus slopes (valais, swiss alps), *Permafrost and Periglacial Processes*, 26(1), 67–83, 2015.

Schädel, C., E. A. Schuur, R. Bracho, B. Elberling, C. Knoblauch, H. Lee, Y. Luo, G. R. Shaver, and M. R. Turetsky, Circumpolar assessment of permafrost c quality and its vulnerability over time using long-term incubation data, *Global Change Biology*, 20(2), 641–652, 2014.

Schrott, L., and O. Sass, Application of field geophysics in geomorphology: advances and limitations exemplified by case studies, *Geomorphology*, 93(1), 55–73, 2008.

Schuur, E., et al., Climate change and the permafrost carbon feedback, *Nature*, 520(7546), 171–179, 2015.

Schuur, E. A., et al., Vulnerability of permafrost carbon to climate change: Implications for the global carbon cycle, *BioScience*, 58(8), 701–714, 2008.

Sellmann, P. V., Geology of the USA CRREL permafrost tunnel, Fairbanks, Alaska, *Tech. rep.*, CRREL DTIC Document, 1967.

Svendsen, J. I., et al., Late Quaternary ice sheet history of northern Eurasia, *Quaternary Science Reviews*, 23(11), 1229–1271, 2004.

Syvitski, J. P., Sediment discharge variability in Arctic rivers: implications for a warmer future, *Polar Research*, 21(2), 323–330, 2002.

Tarasov, L., and W. R. Peltier, Terminating the 100 kyr ice age cycle, *Journal of Geophysical Research: Atmospheres (1984–2012)*, 102(D18), 21,665–21,693, 1997.

Tarnocai, C., J. Canadell, E. Schuur, P. Kuhry, G. Mazhitova, and S. Zimov, Soil organic carbon pools in the northern circumpolar permafrost region, *Global biogeochemical cycles*, 23(2), 2009.

Tesi, T., et al., Massive remobilization of permafrost carbon during post-glacial warming, *Nature Communications*, 7, 2016.

USGS, Gtopo30 global digital elevation model, 1996.

Walker, D., N. Auerbach, and M. Shippert, NDVI, biomass, and landscape evolution of glaciated terrain in northern Alaska , *Polar Record*, 31(177), 169–178, 1995.

Walker, D., W. Gould, H. Maier, and M. Reynolds, The Circumpolar Arctic Vegetation Map: AVHRR-derived base maps, environmental controls, and integrated mapping procedures, *International Journal of Remote Sensing*, 23(21), 4551–4570, 2002.

Wu, T. H., Soil movements on permafrost slopes near fairbanks, alaska, *Canadian Geotechnical Journal*, 21(4), 699–709, 1984.

Yoo, K., R. Amundson, A. M. Heimsath, and W. E. Dietrich, Erosion of upland hillslope soil organic carbon: Coupling field measurements with a sediment transport model, *Global Biogeochemical Cycles*, 19(3), 2005.

Zhang, X., N. A. Drake, J. Wainwright, and M. Mulligan, Comparison of slope estimates from low resolution DEMs: scaling issues and a fractal method for their solution, *Earth*

Surface Processes and Landforms, 24(9), 763–779, 1999.

Zhuang, Q., et al., CO₂ and CH₄ exchanges between land ecosystems and the atmosphere in northern high latitudes over the 21st Century, *Geophysical Research Letters*, 33(17), 2006.

Zimov, S. A., E. A. Schuur, and F. S. Chapin III, Permafrost and the global carbon budget, *Science(Washington)*, 312(5780), 1612–1613, 2006.

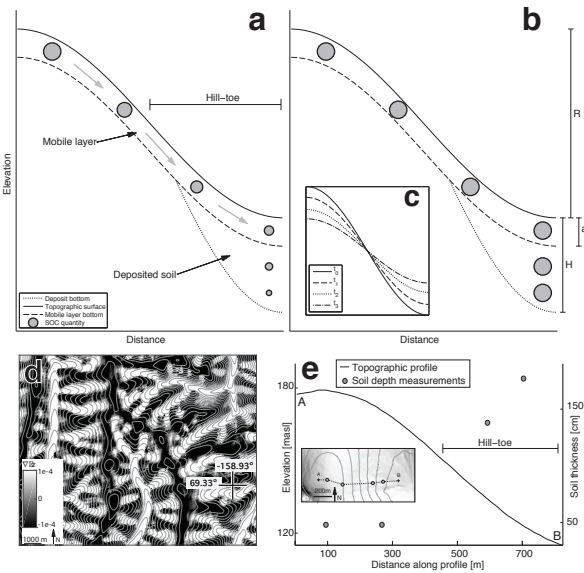


Figure 1: SOC accumulation at hill-toe deposits. (a) A schematic hillslope profile showing soil transport and SOC decomposition. Grey arrows mark the direction of soil flux in the mobile layer. Grey circle on the upper left marks initial SOC quantity, smaller circles downslope indicates a smaller quantity due to SOC decomposition thus illustrating the fate of an initial SOC quantity during transport (regardless of SOC produced along this route). The rate of SOC decomposition in panel a' is high both in the mobile and buried layers so that the initial SOC quantity decreases as it is being transported downslope, and after it is being buried at the hill-toe. (b) Similar to panel a' except that SOC decomposition rate is much lower in both mobile and buried soil such that a larger quantity of SOC remains through transport and deposition. The hillslope relief (R), deposit thickness (H), and active layer thickness (a_t), are marked on the right. (c) Temporal stages in the evolution of a hillslope topography through soil creep (i.e., modeled as linear diffusion). Note the accumulation of deposits at the hill-toe (Following *Berhe et al. [2007]*). (d) A map of topographic curvature values computed from a ~ 50 m DEM of typical hilly soil-mantled terrain affected by permafrost (i.e., HSP terrain) in Alaska. The topography (gray contours ~ 9 m apart) shows that areas of positive curvature are spatially extensive and occur mainly at the lower portion of hill-slopes. (e) Topographic profile (left y-axis) between A to B (in inset) in the Seward Peninsula (Lat, Lon: [65.026660, -166.16686]). The soil thickness (i.e., depth of soil excavation/drilling, right y-axis) at each of the sampling locations shown in the inset is marked by a grey circle. The inset shows a hill-shade map of soil-depth sampling sites, the hillslope extends to the east beyond the margins of the map. Elevation contours (10 m apart) are derived from 5 m IfSAR data [Craun, 2015]. Grey circles mark the location of soil depth measurements. Dashed line between A and B marks the trace of the profile shown in panel e'.

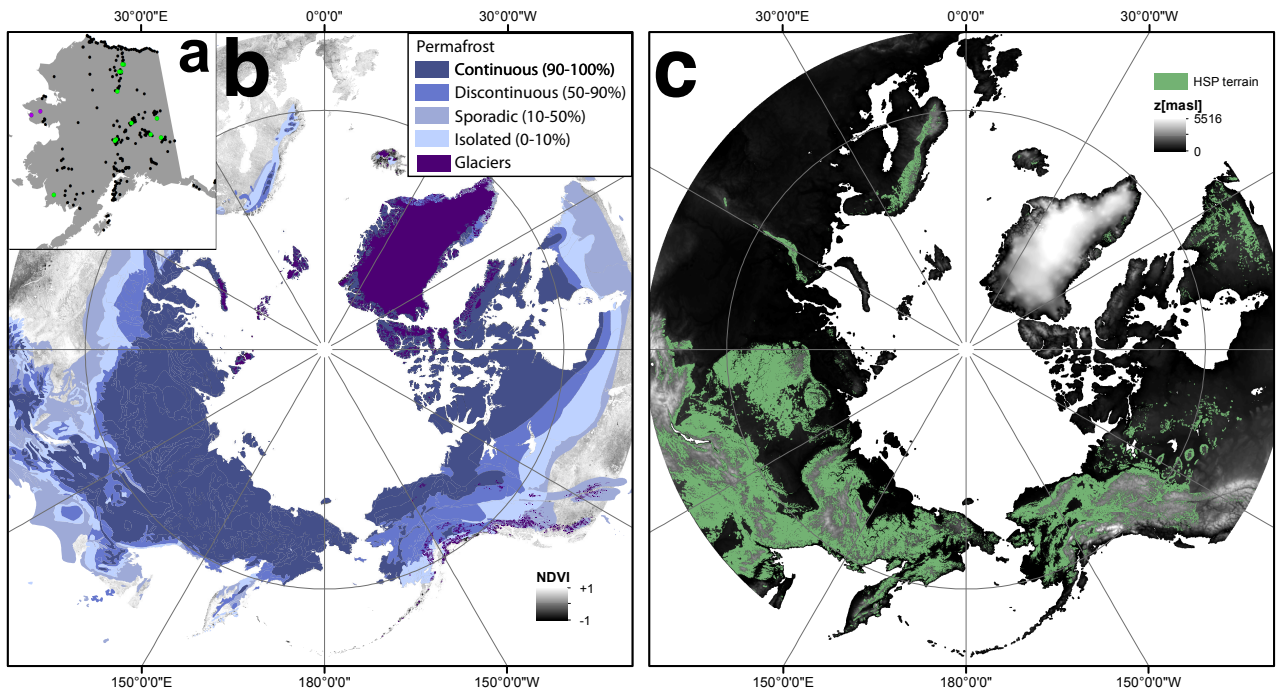


Figure 2: **Classification of hilly soil-mantled permafrost (HSP) terrain.** (a) Soil profile locations in Alaska (N=584, black circles [*Mishra et al., 2017b*]). 16 of these profiles sample permafrost in hill-toe positions (green circles). The locations of our soil depth measurements in the Seward Peninsula are marked in magenta. (b) Permafrost zones map [*Brown et al., 2014*] overlaid on an NDVI map [*CAVM Team, 2003*]. (c) Locations classified as HSP terrain (in green is the maximal extent of HSP terrain, this study) laid over an elevation map [*USGS, 1996*]. The classification of HSP terrain is based on joined analysis of these permafrost, NDVI, and topographic datasets together with the NDVI values associated with the profiles in panel a' (Section 2.3, SI).

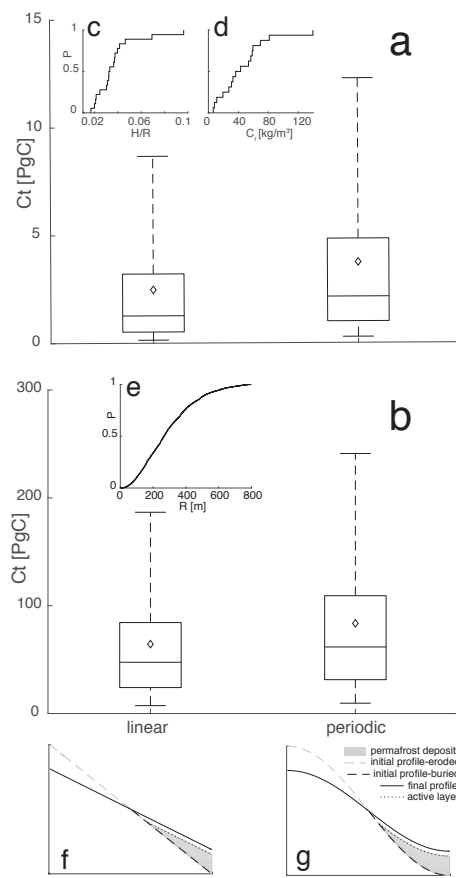


Figure 3: Analysis of SOC mass, soil profiles, hillslope relief, and modeled thickness of hill-toe deposits in Alaska. (a,b) Box-plots of SOC mass (C_t [Pg C]) stored in permafrost hill-toe deposits in Alaska for the two modeled profile geometries. The plots show the cases where deposit depth does (b), and does not (a) scale with relief. Whiskers, box boundary, central line, and diamond symbol mark the [5,95] percentiles, [25,75] percentiles, median and mean, respectively. (c,d,e) Cumulative Distribution Functions (CDFs, P on the y-axis marks probability) from empirical measures of: (c) H/R based on the topographic relief (R) and soil profile depth (H) of the 18 soil depth profiles included this study; (d) Permafrost C content for the 16 profiles with reported C density; (e) local relief of HSP terrain in Alaska (see Section 3.2). (f,g) Illustration of modeled linear and sigmoidal profile geometries, in these models, the hill-toe extends to half of the profile length, and the maximal depth of deposits is determined by H/R .